Journal of the Egyptian Mathematical Society (2016) 24, 656–665

Egyptian Mathematical Society

Journal of the Egyptian Mathematical Society

www.etms-eg.org
www.elsevier.com/locate/joems

Original Article

Lie point symmetries for a magneto couple stress fluid in a porous channel with expanding or contracting walls and slip boundary condition

Rabea El Shennawy Abo Elkhair*

Mathematics Department, Faculty of Science, Al-Azhar University, Nasr City, 11448 Cairo, Egypt

Received 20 December 2015; revised 11 April 2016; accepted 20 April 2016
Available online 17 May 2016

Keywords

Lie point symmetries;
Couple stress fluid;
Porous channel;
Magnetic field;
Expanding and contracting walls;
Slip boundary condition

Abstract In this paper, an incompressible couple stress fluid flow with magnetic field in a porous channel with expanding or contracting walls and slip boundary condition is considered. Lie group analysis and group invariant solutions are obtained, the governing equations are reduced to nonlinear ordinary differential equations. The resulting equations are solved analytically, also this equations are solved by using Adomian method. The graphs for the axial and the normal velocity components and the pressure distribution for different values of the physical and geometric parameters are plotted and discussed. Finally, the comparison between the analytic and Adomian methods is discussed. It is found that for no-slip case $\phi = 0$ the fluid adheres to the walls and axial velocity is maximum at the center of the channel, also by increasing the slip parameter the velocity at the channel walls increases. However, it decreases at center of the channel by increasing slip parameter.

2010 Mathematical Subject Classification: 76D05; 76M60; 76M99; 76S05; 76W05

1. Introduction

Studying of a couple stress fluid is an important to understanding some physical problems, because it have the mechanism to characterize rheologically complex fluids such as liquid crystals, colloidal fluids, animal and human blood and lubrication. The micro-continuum theory of couple stress fluid proposed by Stokes [1], some theoretical studies [2–4] considered the blood couple stress fluid flow as a non-Newtonian fluid flow for its properties. Sometimes the couple-stress fluid considered as a special case of a non-Newtonian fluid which is purposed to take the effect of the particle size into account. Moreover, the couple stress fluid model is one of the numerous models that proposed to show response characteristics of non-Newtonian fluids. The constitutive equations for couple stress fluid models is very complex and involving number of parameters, also

* Tel.: +201226338195.
E-mail address: elkhair33@yahoo.com
Peer review under responsibility of Egyptian Mathematical Society.

Production and hosting by Elsevier

http://dx.doi.org/10.1016/j.joems.2016.04.001

the out coming couple stress equations lead to boundary value problems with higher order than the Navier–Stokes. Shehawey and Mekheimer [5] proposed applications of the couple stress model to biomechanics problems of peristaltic transport and blood flow in the microcirculation by Mekheimer [6]. Recently many authors have studied the effect of couple stress on different problems (see for example: Samuel et al. [7] and Turkyilmazoglu [8]).

There are some applications in biophysical flow through porous channels with expanding or contracting walls, such as air and blood circulation in the respiratory system, pulsating diaphragms, artificial dialysis, filtration, blood flow and binary gas diffusion. For these applications many authors studied the flow through a porous channels for different models such as analysis of some magnetohydrodynamic flows of third order fluid [9], non-Newtonian nanofluids flow through a porous medium between two coaxial cylinders with heat transfer and variable viscosity [10] and magnetohydrodynamic flow of water/ethylene glycol based nanofluids with natural convection [11]. An unsteady flows in a semi-infinite contracting or expanding pipe studied firstly by Uchida and Aoki [12]. Also, Ohki [13] investigated the unsteady flow in a porous, elastic, circular tube with contracting or expanding walls in an axial direction. A series solution to an unsteady flow in a contracting or expanding pipe is discussed by Bujurke et al. [14]. Numerical and asymptotical solutions for moderate large Reynolds numbers obtained by Majdalani and Zhou [15]. Also, Dinarvand [16] studied viscous flow with low seepage Reynolds number through slowly expanding or contracting porous walls: a model for transport of biological fluids through vessels.

No-slip condition was not have longer valid at the permeable surface, Beavers and Joseph [17] reported mass flux experiments and proved that a non-zero tangential (slip) velocity on a permeable boundary surface has effect. Some experimental and theoretical studies stated that slip condition could not be ruled out as an important element to understanding of certain characteristic flow [18]. Using a statistical approach, Saffman [19] derived the slip velocity form. Isenberg [20] posited slip condition in his study of blood flow in capillary tubes. Recently, Zhang and Jia [21] studied the first and second order Navier–Stokes equations accurate slip boundary conditions for describing the two-dimensional gaseous steady laminar flow between two plates. Ramos [22] obtained an asymptotic analytical solution for an incompressible fluid flow in channel with a slip length that depended on the pressure and/or the axial pressure gradient. Also some authors studied the effect of slip condition on some difference problems such that peristaltic flow of Jeffrey fluid model in a three dimensional rectangular duct [23], flow of non-Newtonian fluid with variable viscosity through a porous medium in an inclined channel [24] and non-Newtonian MHD fluid in porous space [25].

Lie group analysis (Lie point symmetries) method is an important method for find exact solutions of ordinary and partial differential equations by using transformations groups (similarity transformations) which introduced firstly by Sophus Lie [26]. The groups of continuous transformations that leave a given family of invariant equations are defined as the symmetries (isovector fields). The symmetry transformation is reduced the independent variables from n to $n-1$ variables [27]. Many authors have been obtained the exact solutions for some problems in fluid mechanics by using Lie group analysis method. Boutros et al. [28] studied Lie-group method solution for two-dimensional viscous flow for an expanding or contracting walls with weak permeability. Mekheimer et al. obtained the exact solutions for a couple stress fluid with heat transfer, an electrically conducting Jeffrey fluid, micro-polar fluid through a porous medium and hydro-magnetic Maxwell fluid through a porous medium [29–32], also Shahzad et al. [33] use this method to find the analytical solution of a micro-polar fluid.

The main goal of this paper is to find the analytical and approximate solutions for a magneto couple stress fluid flow in a porous channel with expanding and contracting walls using duple perturbation and Adomian methods. In Section 3, the basic roles of the Lie group analysis method are given and used to calculate the isovector field of our equations. The analytical solution (duple perturbation) corresponding to the nonlinear ordinary differential equation obtained in Section 4. Adomian decomposition method is used to obtain the solution of our ODE in Section 5. Finally, the graphs for velocity components and the pressure distribution presented for different values of the physical and geometric parameters are plotted and discussed.

2. Equations of motion

Consider an unsteady two-dimensional motion of an incompressible magneto couple stress fluid in a porous semi-infinite channel with expanding or contracting walls.

The distance $2a(t)$ between channel's walls is very small with respect to the width and length of the channel. The channel is closed from one end by a complicated solid membrane. Walls have equal permeability V_w and expand or contract uniformly at a time-dependent rate $\dot{a}(t)$, as shown in Fig. 1. We take $\widehat{x}$ and $\widehat{y}$ to be co-ordinate axes parallel and perpendicular to the channel walls and assume $\widehat{u}$ and $\widehat{v}$ to be the velocity components in the $\widehat{x}$ and $\widehat{y}$ directions respectively. The governing equations are expressed as follows,

$$\begin{cases} \dfrac{\partial \widehat{u}}{\partial \widehat{x}} + \dfrac{\partial \widehat{v}}{\partial \widehat{y}} = 0, \\ \rho\left(\dfrac{\partial \widehat{u}}{\partial t} + \widehat{u}\dfrac{\partial \widehat{u}}{\partial \widehat{x}} + \widehat{v}\dfrac{\partial \widehat{u}}{\partial \widehat{y}}\right) = -\dfrac{\partial \widehat{p}}{\partial \widehat{x}} + \mu\nabla^2\widehat{u} - \eta\nabla^4\widehat{u} - \sigma B_0^2\widehat{u}, \\ \rho\left(\dfrac{\partial \widehat{u}}{\partial t} + \widehat{v}\dfrac{\partial \widehat{v}}{\partial \widehat{x}} + \widehat{v}\dfrac{\partial \widehat{v}}{\partial \widehat{y}}\right) = -\dfrac{\partial \widehat{p}}{\partial \widehat{y}} + \mu\nabla^2\widehat{v} - \eta\nabla^4\widehat{v}, \end{cases} \tag{1}$$

where $\nabla^2 = \dfrac{\partial^2}{\partial \widehat{x}^2} + \dfrac{\partial^2}{\partial \widehat{y}^2}$, $\nabla^4 = \nabla^2(\nabla^2)$, and $\widehat{p}(\widehat{x}, \widehat{y})$ is the pressure distribution. Here ρ, μ, σ, B_0 and η are mass density, coefficient of viscosity, electrical conductivity of the fluid, magnetic field and couple-stress parameter.

The boundary conditions of our problem will be

$$\begin{aligned} &(i) \quad \frac{\partial^2 \widehat{u}}{\partial \widehat{y}^2} = 0, \quad \widehat{u} = -\frac{\sqrt{k}}{\iota}\frac{\partial \widehat{u}}{\partial \widehat{y}}, \quad \widehat{v} = -V_w = -A\,\dot{a}, \quad at \\ &\quad \widehat{y} = a(t), \\ &(ii) \quad \frac{\partial^3 \widehat{u}}{\partial \widehat{y}^3} = 0, \quad \frac{\partial \widehat{u}}{\partial \widehat{y}} = 0, \quad \widehat{v} = 0, \quad at \quad \widehat{y} = 0, \\ &(iii) \quad \widehat{u} = 0, \quad at \quad \widehat{x} = 0, \end{aligned} \tag{2}$$

where ι is a dimensionless constant which depends on the pore size of the permeable material, k is the specific permeability of the porous medium. Take the stream function $\widehat{\psi}(\widehat{x}, \widehat{y}, t)$ such

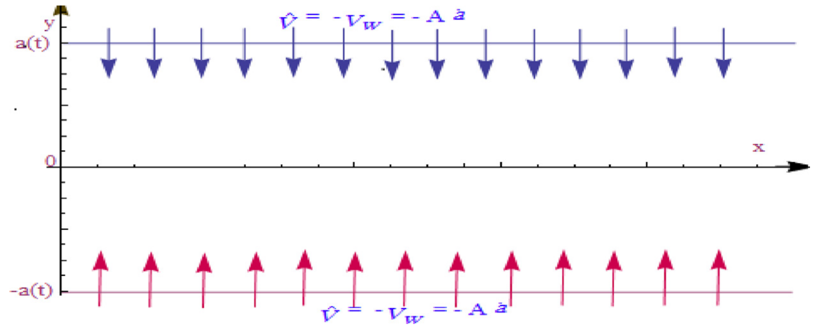

Fig. 1 Geometry of the problem.

that

$$\widehat{u}=\frac{\partial\widehat{\psi}}{\partial\widehat{y}},\quad \widehat{v}=-\frac{\partial\widehat{\psi}}{\partial\widehat{x}}, \tag{3}$$

which satisfies the continuity equation identically.

If we introduce the dimensionless perpendicular coordinate $y=\frac{\widehat{y}}{a(t)}$, Eq. (3) becomes

$$\widehat{u}=\frac{1}{a}\frac{\partial\widehat{\psi}}{\partial y},\quad \widehat{v}=-\frac{\partial\widehat{\psi}}{\partial\widehat{x}}. \tag{4}$$

Substitute from (4) into (1), then we have:

$$\begin{aligned}
&a^2\widehat{\psi}_{yt}-a\,\dot{a}y\widehat{\psi}_{yy}-a\,\dot{a}\widehat{\psi}_y+a\widehat{\psi}_y\widehat{\psi}_{\widehat{x}y}-a\widehat{\psi}_{\widehat{x}}\widehat{\psi}_{yy}+\frac{a^3}{\rho}\widehat{p}_{\widehat{x}}\\
&\quad-\nu(a^2\widehat{\psi}_{\widehat{x}\widehat{x}y}+\widehat{\psi}_{yyy})+\frac{\eta}{a^2\rho}(a^4\widehat{\psi}_{\widehat{x}\widehat{x}\widehat{x}\widehat{x}y}+\widehat{\psi}_{yyyyy})\\
&\quad-\frac{1}{\rho}\sigma B_0^2a^2\widehat{\psi}_y=0,\\
&\quad-a^2\widehat{\psi}_{\widehat{x}t}+a\,\dot{a}y\widehat{\psi}_{\widehat{x}y}-a\widehat{\psi}_y\widehat{\psi}_{\widehat{x}\widehat{x}}+a\widehat{\psi}_{\widehat{x}}\widehat{\psi}_{\widehat{x}y}+\frac{a}{\rho}\widehat{p}_y\\
&\quad+\nu(a^2\widehat{\psi}_{\widehat{x}\widehat{x}\widehat{x}}+\widehat{\psi}_{\widehat{x}yy})\\
&\quad-\frac{\eta}{a^2\rho}(a^4\widehat{\psi}_{\widehat{x}\widehat{x}\widehat{x}\widehat{x}\widehat{x}}+\widehat{\psi}_{\widehat{x}yyyy})=0.
\end{aligned} \tag{5}$$

By using the following dimensionless parameters

$$\begin{aligned}
&u=\frac{\widehat{u}}{V_w},\quad v=\frac{\widehat{v}}{V_w},\quad x=\frac{\widehat{x}}{a(t)},\quad \widehat{t}=\frac{tV_w}{a},\quad \psi=\frac{\widehat{\psi}}{aV_w},\\
&p=\frac{\widehat{p}}{\rho V_w^2},\quad \alpha=\frac{a\dot{a}}{\nu},
\end{aligned} \tag{6}$$

the system (5) becomes

$$\begin{aligned}
E_1&=\psi_{y\widehat{t}}+\psi_y\psi_{xy}-\psi_x\psi_{yy}+p_x-\frac{1}{R_e}((\alpha-M^2)\psi_y\\
&\quad+\alpha y\psi_{yy}+\psi_{xxy}+\psi_{yyy})\\
&\quad+\frac{1}{\gamma^2R_e}(\psi_{xxxxy}+\psi_{yyyyy})=0,\\
E_2&=\psi_{x\widehat{t}}+\psi_y\psi_{xx}-\psi_x\psi_{xy}-p_y-\frac{1}{R_e}(\alpha y\psi_{xy}+\psi_{xxx}+\psi_{xyy})\\
&\quad+\frac{1}{\gamma^2R_e}(\psi_{xxxxx}+\psi_{xyyyy})=0,
\end{aligned} \tag{7}$$

where $R_e=\frac{aV_w}{\nu}$ is the permeation Reynolds number, $M^2=\frac{\sigma B_0^2a^2}{\mu}$ is the Hartman number and $\gamma^2=\frac{\mu a^2}{\eta}$ is the dimensionless couple stress parameter.

The wall permeance or injection coefficient A is defined as $A=\frac{Re}{a}$, it is a measure of wall permeability.

From (4) and (6), we can write

$$u=\frac{\partial\psi}{\partial y},\quad v=-\frac{\partial\psi}{\partial x}. \tag{8}$$

The boundary conditions (2) will be

$$\begin{array}{llll}
(i) & \psi_{yyy}=0,\quad \psi_y=-\phi\psi_{yy},\quad \psi_x=1 & at & y=1,\\
(ii) & \psi_{yyyy}=0,\quad \psi_{yy}=0,\quad \psi_x=0 & at & y=0,\\
(iii) & \psi_y=0,\quad at\quad x=0. & &
\end{array} \tag{9}$$

where $\phi=\frac{\sqrt{k}}{\iota a}$ is the slip coefficient. From a physical standpoint, the idealization is based on a decelerating wall dilation rate that follows a plausible model according to which

$$a\,\dot{a}=\ constant. \tag{10}$$

So, the rate of dilation decreases as the channel height increases.

Since $\alpha=\frac{a\dot{a}}{\nu}$, then, integration of (10) yields

$$\frac{a}{a_0}=\sqrt{1+\frac{2\alpha\nu t}{a_0^2}}, \tag{11}$$

where a_0 is the initial value of the channel height.

3. Lie group analysis and isovector fields

To obtain the analytical solution, we apply Lie group analysis method on equations of the system (7). For this we write

$$\begin{cases} x_i^*=x_i+\epsilon\,\xi_i(x_j,u_\beta)+\mathbf{o}(\epsilon^2),\\ u_\alpha^*=u_\alpha+\epsilon\,\eta_\alpha(x_j,u_\beta)+\mathbf{o}(\epsilon^2),\end{cases}\quad i,j=1,2,3,\quad \alpha,\beta=1,2, \tag{12}$$

as the infinitesimal Lie point transformations. We have assumed that the system in Eq. (7) is invariant under the transformations given in Eq. (12). The corresponding infinitesimal generator of Lie groups is given by

$$X = \xi_i \frac{\partial}{\partial x_i} + \eta_\alpha \frac{\partial}{\partial u_\alpha}, \tag{13}$$

with summation convention over the repeated index and $x_1 \equiv x,\ x_2 \equiv y,\ x_3 \equiv \hat{t},\ u_1 \equiv \psi,\ u_2 \equiv p$. The coefficients $\xi_1, \xi_2, \xi_3, \eta_1$ and η_2 are the functions of all independent and dependent variables. There coefficients are the components of the infinitesimals symmetries corresponding to $x, y, \hat{t}, \psi$ and p, respectively to be determined from the invariance conditions:

$$\mathrm{Pr}^{(5)}\, X(E_a)|_{E_a=0} = 0, \quad a = 1, 2, \tag{14}$$

where $E_a = 0,\ i = 1, 2$ represent the system of Eq. (7) and $\mathrm{Pr}^{(5)}$ is the fifth prolongation of the isovector field X.

Since the system (7) is of order five, then our prolongation will be in the form

$$\begin{aligned}
\mathrm{Pr}^{(1)} X &= X + \eta_{\alpha i} \frac{\partial}{\partial u_{\alpha,i}},\\
\mathrm{Pr}^{(2)} X &= \mathrm{Pr}^{(1)} X + \eta_{\alpha ij} \frac{\partial}{\partial u_{\alpha,ij}},\\
\mathrm{Pr}^{(3)} X &= \mathrm{Pr}^{(2)} X + \eta_{\alpha ijk} \frac{\partial}{\partial u_{\alpha,ijk}},\\
\mathrm{Pr}^{(4)} X &= \mathrm{Pr}^{(3)} X + \eta_{\alpha ijkl} \frac{\partial}{\partial u_{\alpha,ijkl}},\\
\mathrm{Pr}^{(5)} X &= \mathrm{Pr}^{(4)} X + \eta_{\alpha ijklm} \frac{\partial}{\partial u_{\alpha,ijklm}},
\end{aligned} \tag{15}$$

where

$$\begin{aligned}
\eta_{\alpha i} &= D_i[\eta_\alpha - \xi_j u_{\alpha,j}] + \xi_j u_{\alpha,ji},\\
\eta_{\alpha ij} &= D_{ij}[\eta_\alpha - \xi_k u_{\alpha,k}] + \xi_k u_{\alpha,kij},\\
\eta_{\alpha ijk} &= D_{ijk}[\eta_\alpha - \xi_l u_{\alpha,l}] + \xi_l u_{\alpha,lijk},\\
\eta_{\alpha ijkl} &= D_{ijkl}[\eta_\alpha - \xi_m u_{\alpha,m}] + \xi_m u_{\alpha,mijkl},\\
\eta_{\alpha ijklm} &= D_{ijklm}[\eta_\alpha - \xi_n u_{\alpha,n}] + \xi_n u_{\alpha,nijklm},
\end{aligned} \tag{16}$$

and the operator $D_{i_1 i_2 \ldots i_s}$ is called the *total derivative* (*Hash operator*) and have the following form:

$$\begin{aligned}
D_i = {} & \frac{\partial}{\partial x_i} + u_{\alpha,i} \frac{\partial}{\partial u_\alpha} + u_{\alpha,ij} \frac{\partial}{\partial u_{\alpha,j}} + u_{\alpha,ijk} \frac{\partial}{\partial u_{\alpha,jk}} + u_{\alpha,ijkl} \frac{\partial}{\partial u_{\alpha,jkl}}\\
& + u_{\alpha,ijklm} \frac{\partial}{\partial u_{\alpha,jklm}} + u_{\alpha,ijklmn} \frac{\partial}{\partial u_{\alpha,jklmn}},
\end{aligned} \tag{17}$$

where $D_{ij} = D_i(D_j) = D_j(D_i) = D_{ji}$ and $u_{\alpha,i} = \frac{\partial u_\alpha}{\partial x_i}$.

Expanding the system of Eq. (14) with the aid of *Mathematica programm*, along with the original system of Eq. (7) to eliminate p_x, p_y and setting the coefficients involving $\psi_y, \psi_x, \psi_{\hat{t}}, \psi_{yy}, \psi_{xx}, \psi_{xy}, \psi_{x\hat{t}}, \psi_{y\hat{t}}, \psi_{yyy}, \psi_{xyy}, \psi_{xxy}, \psi_{xxx}, \psi_{yyyy}, \psi_{xyyy}, \psi_{xxyy}, \psi_{xxxy}, \psi_{xxxx}, \psi_{yyyyy}, \psi_{xyyyy}, \psi_{xxyyy}, \psi_{xxxyy}, \psi_{xxxxy}, \psi_{xxxxx}$ and various products to zero give rise the essential set of over-determined equations. Solving these set of determining equations we obtain the required components of isovector field

Table 1 Table of commutators of the basis operators.

	X_1	X_2	X_3	$X_4(a_4)$	$X_5(a_5)$
X_1	0	0	0	0	0
X_2	0	0	$-\frac{\alpha}{R_e} X_3$	$X_4(a_4')$	$X_5(a_5')$
X_3	0	$\frac{\alpha}{R_e} X_3$	0	0	0
$X_4(a_4)$	0	$-X_4(a_4')$	0	0	0
$X_5(a_5)$	0	$-X_5(a_5')$	0	0	0

as follows:

$$\begin{aligned}
&\xi_1 = a_1(\hat{t}), \quad \xi_2 = a_2\, e^{-\frac{\alpha \hat{t}}{R_e}}, \quad \xi_3 = a_3,\\
&\eta_1 = a_4(\hat{t}) + y\, a_1'(\hat{t}), \quad \eta_2 = a_5(\hat{t}) + x\left(\frac{1}{R_e} a_1'(\hat{t}) - a_1''(\hat{t})\right).
\end{aligned} \tag{18}$$

If we take $a_1(\hat{t}) = a_1$ we get

$$\begin{aligned}
&\xi_1 = a_1, \quad \xi_2 = a_2\, e^{-\frac{\alpha \hat{t}}{R_e}}, \quad \xi_3 = a_3, \quad \eta_1 = a_4(\hat{t}),\\
&\eta_2 = a_5(\hat{t}),
\end{aligned} \tag{19}$$

where $a_i, i = 1, 2, 3$ are arbitrary constants and $a_4(\hat{t}), a_5(\hat{t})$ are arbitrary functions of the variable $\hat{t}$ only. Therefore, the equations admit a five parameters Lie group of transformations corresponding to the arbitrary constants $a_1, a_2\ a_3$ and arbitrary functions a_4, a_5. The infinitesimal generator of Lie groups can be written in the form of Lie algebra as the following:

$$X = \sum_{i=1}^{5} a_i X_i, \tag{20}$$

where

$$\begin{aligned}
&X_1 = \frac{\partial}{\partial x}, \quad X_2 = \frac{\partial}{\partial \hat{t}}, \quad X_3 = e^{-\frac{\alpha}{R_e}\hat{t}} \frac{\partial}{\partial y}, \quad X_4 = a_4(\hat{t}) \frac{\partial}{\partial \psi},\\
&X_5 = a_5(\hat{t}) \frac{\partial}{\partial p}.
\end{aligned} \tag{21}$$

The one-parameter group generated by X_1 and X_2 consists of translations, whereas other symmetries are non-trivial. The commutator table of the symmetries is given below, where the entry in the ith row and jth column is defined as $[X_i, X_j] = X_i X_j - X_j X_i$, see Table 1.

The solutions $\psi = \psi(x, y, \hat{t})$ and $p = p(x, y, \hat{t})$, are invariant under the symmetry (13) if

$$\begin{aligned}
&\phi_\psi = X(\psi - \psi(x, y, \hat{t})) = 0 \quad \textit{when} \quad \psi = \psi(x, y, \hat{t})\\
&\phi_p = X(p - p(x, y, \hat{t})) = 0 \quad \textit{when} \quad p = p(x, y, \hat{t})
\end{aligned} \tag{22}$$

For X_2, the characteristic has the components $\phi_\psi = -\psi_{\hat{t}} = 0$, $\phi_p = -p_{\hat{t}} = 0$. Therefore, the general solutions of the invariant surface conditions (22) are

$$\psi = h(y)\, H(x, y), \qquad p = p(x, y). \tag{23}$$

Substitution from (23) into the first equation in (7) yields

$$BR_e\left(\frac{d^5h}{dy^5}+5\frac{H_y}{H}\frac{d^4h}{dy^4}\right)-\left(1-10BR_e\frac{H_{yy}}{H}\right)\frac{d^3h}{dy^3}$$
$$-\left(3\frac{H_y}{H}+\alpha y+R_e(hH_x-10B\frac{H_{yyy}}{H})\right)\frac{d^2h}{dy^2}$$
$$-\left(2\alpha y\frac{H_y}{H}+3\frac{H_{yy}}{H}-5BR_e\frac{H_{yyyy}}{H}+\alpha-M^2+\frac{H_{xx}}{H}\right.$$
$$\left.-BR_e\frac{H_{xxxx}}{H}+R_eh\frac{H_xH_y}{H}-R_ehH_{xy}\right)\frac{dh}{dy}$$
$$+R_eH_x\left(\frac{dh}{dy}\right)^2-\left((\alpha-M^2)\frac{H_y}{H}+\alpha y\frac{H_{yy}}{H}+\frac{H_{yyy}}{H}\right.$$
$$\left.-BR_e\frac{H_{yyyyy}}{H}+\frac{H_{xxy}}{H}-BR_e\frac{H_{xxxxy}}{H}\right)h$$
$$-R_e\left(\frac{H_xH_{yy}}{H}-\frac{H_yH_{xy}}{H}\right)h^2+\frac{R_e}{H}p_x=0, \tag{24}$$

which can be rewritten as

$$BR_e(\frac{d^5h}{dy^5}+5k_2\frac{d^4h}{dy^4})-(1-10BR_ek_6)\frac{d^3h}{dy^3}$$
$$-(3k_2-10BR_ek_{10}+\alpha y+R_ehk_1)\frac{d^2h}{dy^2}$$
$$-(2\alpha yk_2+3k_6-5BR_ek_{11}+\alpha-M^2+k_5-BR_ek_{12}$$
$$+R_e(k_3-k_4)h)\frac{dh}{dy}+R_ek_1\left(\frac{dh}{dy}\right)^2$$
$$-((\alpha-M^2)k_2+\alpha yk_6+k_{10}-BR_ek_{13}+k_9-BR_ek_{14})h$$
$$-R_e(k_7-k_8)h^2+\frac{R_e}{H}p_x=0, \tag{25}$$

where

$$k_1=H_x,\quad k_2=\frac{H_y}{H},\quad k_3=\frac{H_xH_y}{H},\quad k_4=H_{xy},\quad k_5=\frac{H_{xx}}{H},$$
$$k_6=\frac{H_{yy}}{H},$$
$$k_7=\frac{H_yH_{xy}}{H},\quad k_8=\frac{H_xH_{yy}}{H},\quad k_9=\frac{H_{xxy}}{H},\quad k_{10}=\frac{H_{yyy}}{H},$$
$$k_{11}=\frac{H_{yyyy}}{H},$$
$$k_{12}=\frac{H_{xxxx}}{H},\ k_{13}=\frac{H_{yyyyy}}{H},\ k_{14}=\frac{H_{xxxxy}}{H},\quad B=\frac{1}{\gamma^2R_e} \tag{26}$$

Since h is a function of y only, whereas H and p are functions of x and y, thus from Eq. (25) we conclude that each of $K_i, i=1,2,\ldots,14$ must be a constant or function of y only to obtain an expression in the single variable y.

Solution of $H_x=K_1$ in (26) gives

$$H(x,y)=xk_1(y)+C_1(y). \tag{27}$$

Substitution from (27) into the first equation of (23) will give

$$\psi=(xk_1(y)+C_1(y))h(y). \tag{28}$$

By using the boundary conditions (9) we get

$$C_1(y)h(y)=C_2, \tag{29}$$

where C_2 is a constant. Substitution from (29) into (28), gives

$$\psi=xG(y)+C_2, \tag{30}$$

where $G(y)=k_1(y)h(y)$, substitution from the second equation of (23) and (30) into the first equation in (7), yields

$$R_e\frac{\partial p}{\partial x}=x\left(-BR_e\frac{d^5G}{dy^5}+\frac{d^3G}{dy^3}+(R_eG+\alpha y)\frac{d^2G}{dy^2}\right.$$
$$\left.+(\alpha-M^2)\frac{dG}{dy}-R_e\left(\frac{dG}{dy}\right)^2\right). \tag{31}$$

Substitution from (27) and (30) into the last term of (25), yields $C_1=0$. Then $H(x,y)=xk_1(y)$, which satisfies the remaining $k_i=1,2,\ldots,14$.

And the stream function take the form

$$\psi=xG(y). \tag{32}$$

From (32) into (8) we get

$$u=x\frac{dG}{dy},\qquad v=-G. \tag{33}$$

Substitution from (32) into the second equation in (7) and then differentiating with respect to x, yields

$$p_{xy}=0. \tag{34}$$

Using (32) into the first equation in (7), then differentiating with respects to y and using (34), we get

$$\frac{d^6G}{dy^6}-\gamma^2\frac{d^4G}{dy^4}-\alpha\gamma^2(y\frac{d^3G}{dy^3}+2\frac{d^2G}{dy^2})+\gamma^2M^2\frac{d^2G}{dy^2}$$
$$-R_e\gamma^2(G\frac{d^3G}{dy^3}-\frac{dG}{dy}\frac{d^2G}{dy^2})=0. \tag{35}$$

The boundary conditions (9) will be

$$\begin{array}{llll}(i) & \frac{d^3G}{dy^3}=0, & \frac{dG}{dy}=-\phi\frac{d^2G}{dy^2}, & G=1,\quad at\quad y=1\\ (ii) & \frac{d^4G}{dy^4}=0, & \frac{d^2G}{dy^2}=0, & G=0\quad at\quad y=0.\end{array} \tag{36}$$

4. Analytical solution

The non-linear differential equation (35) with the boundary conditions (36) will solve analytical by using double perturbations method. For small R_e and α, assume

$$\begin{aligned}G&=G_0+R_eG_1+\mathbf{O}(R_e^2),\\ G_0&=G_{00}+\alpha G_{01}+\mathbf{O}(\alpha^2),\\ G_1&=G_{10}+\alpha G_{11}+\mathbf{O}(\alpha^2).\end{aligned} \tag{37}$$

Substitution from (37) into (35),

$$\frac{d^6G_{00}}{dy^6}-\gamma^2\frac{d^4G_{00}}{dy^4}+\gamma^2M^2\frac{d^2G_{00}}{dy^2}=0,$$
$$\frac{d^6G_{01}}{dy^6}-\gamma^2\frac{d^4G_{01}}{dy^4}+\gamma^2M^2\frac{d^2G_{01}}{dy^2}-\gamma^2\left(y\frac{d^3G_{00}}{dy^3}+2\frac{d^2G_{00}}{dy^2}\right)=0,$$
$$\frac{d^6G_{10}}{dy^6}-\gamma^2\frac{d^4G_{10}}{dy^4}+\gamma^2M^2\frac{d^2G_{10}}{dy^2}$$

$$-\gamma^2\left(G_{00}\frac{d^3G_{00}}{d\,y^3}-\frac{dG_{00}}{d\,y}\frac{d^2G_{00}}{d\,y^2}\right)=0,$$
$$\frac{d^6G_{11}}{d\,y^6}-\gamma^2\frac{d^4G_{11}}{d\,y^4}+\gamma^2M^2\frac{d^2G_{11}}{d\,y^2}-\gamma^2\left(G_{01}\frac{d^3G_{00}}{d\,y^3}+G_{00}\frac{d^3G_{01}}{d\,y^3}\right.$$
$$\left.-\frac{dG_{00}}{d\,y}\frac{d^2G_{01}}{d\,y^2}-\frac{dG_{01}}{d\,y}\frac{d^2G_{00}}{d\,y^2}\right)=0, \tag{38}$$

Solutions of (38) with its boundary conditions are

$$G_{00}(y)=a_1\sinh[ry]+a_2\sinh[sy]+a_3y,$$
$$G_{01}(y)=b_1\sinh[ry]+b_2\sinh[sy]+b_3y+\frac{\gamma^2a_1}{4(2r^2-\gamma^2)}\left(y^2\sinh[ry]-\frac{(6r^2-\gamma^2)}{r(2r^2-\gamma^2)}y\cosh[ry]\right)$$
$$+\frac{\gamma^2a_2}{4(2s^2-\gamma^2)}(y^2\sinh[sy]-\frac{(6s^2-\gamma^2)}{s(2s^2-\gamma^2)}y\cosh[sy]),$$
$$\begin{aligned}G_{10}(y)=\;&(8r\gamma^4(-25M^2+4\gamma^2)(-2a_2a_3M^2\gamma^2((-36M^2\\&+11s^2)y\gamma^2(-4M^2+\gamma^2)\cosh[sy]\\&+s(54s^2\gamma^2-16M^4y^2\gamma^2+\gamma^4(7+y^2(-2s^2))\\&+4M^2(46s^2+\gamma^2(y^2(\gamma^2+2s^2)\\&-3)))\sinh[sy])+16s(-4M^2+\gamma^2)^2(c_3y\\&+M^2\gamma^2(c_1\sinh[ry]+c_2\sinh[sy])))\\&-32a_1a_2M^2\gamma^6(-4M^2+\gamma^2)(9(-r+s)\gamma^4\\&+13(r+s)\gamma^2\sqrt{-4M^2\gamma^2+\gamma^4}\\&+4M^2(9(r-s)\gamma^2+5(r+s)\sqrt{-4M^2\gamma^2+\gamma^4}))\\&\sinh[(-r+s)y]\\&-a_1(16a_3M^2s\gamma^6(-25M^2+4\gamma^2)(-2y\gamma^2(-4M^2+\gamma^2)\\&(6M^2(1+2\gamma)\\&-r^2(5+6\gamma))\cosh[ry]-r(16M^4y^2\gamma^2\\&+9\gamma^2(1+2\gamma)\sqrt{-4M^2\gamma^2+\gamma^4}\\&+\gamma^5(12+y^2\gamma)+\gamma^4(8+y^2\sqrt{-4M^2\gamma^2+\gamma^4})\\&-4M^2((5+18\gamma)\sqrt{-4M^2\gamma^2+\gamma^4}\\&+\gamma^2(8+12\gamma+2y^2\gamma^2+y^2\sqrt{-4M^2\gamma^2+\gamma^4})))\sinh[ry])\\&+16a_2M^2\gamma^6(-4M^2+\gamma^2)\\&(9(r+s)\gamma^4+13(-r+s)\gamma^2\sqrt{-4M^2\gamma^2+\gamma^4}\\&+4M^2(-9(r+s)\gamma^2+5(-r+s)\\&\sqrt{-4M^2\gamma^2+\gamma^4}))\sinh[(r+s)y]))\big(16r^3s^3\gamma^4\\&(-4M^2+\gamma^2)^2(-25M^2+4\gamma^2)\big)^{-1},\end{aligned} \tag{39}$$

where $r, s, a_1, a_2, a_3, b_1, b_2, b_3, c_1, c_2$ and c_3 are computing from the boundary conditions in (36) and showing in Appendix A.

Then, solution of (35) with the boundary conditions (36) will be

$$G(y)=G_{00}+\alpha G_{01}+R_eG_{10}, \tag{40}$$

where we neglected the term that containing αR_e .

The velocity components u and v can be obtained from Eq. (33). To determine the normal pressure drop, substitute from (30) into the second equation in (7), we get

$$P_y=-(G\,G_y+\frac{1}{R_e}(G_{yy}+\alpha\,y\,G_y-\frac{1}{\gamma^2}\,G_{yyyy})). \tag{41}$$

We can determine the normal pressure distribution, if we integrate (41) with the boundary conditions given by Eq. (36) and let P_c be the centerline pressure, hence

$$\int_{p_c}^{p(y)}d\,p=-\int_0^y\left(G\,G_y+\frac{1}{R_e}(G_{yy}+\alpha\,y\,G_y-\frac{1}{\gamma^2}\,G_{yyyy})\right)d\,y. \tag{42}$$

The resulting normal pressure drop will be

$$\begin{aligned}\Delta p_n&=p(y)-p_c\\&=\frac{1}{2}G^2(0)+\frac{1}{R_e}(G_y(0)-\frac{1}{\gamma^2}G_{yyy}(0))\\&\quad-\left(\frac{1}{2}G^2+\frac{1}{R_e}(G_y+\alpha y\,G-\frac{1}{\gamma^2}G_{yyy}-\alpha\int_0^y G\,d\,y)\right).\end{aligned} \tag{43}$$

To determine the axial pressure drop, substitute from (30) into the first equation in (7), we get

$$P_x=x\left(G(G_y+G_{yy})+\frac{1}{R_e}((\alpha-M^2)G_y+\alpha\,y\,G_{yy}+G_{yyy}-G_y^2-\frac{1}{\gamma^2}\,G_{yyyyy})\right). \tag{44}$$

The resulting axial pressure will be

$$\Delta p_a=\frac{x^2}{2}\left(G(G_y+G_{yy})+\frac{1}{R_e}\left((\alpha-M^2)G_y+\alpha\,y\,G_{yy}+G_{yyy}-G_y^2-\frac{1}{\gamma^2}\,G_{yyyyy}\right)\right). \tag{45}$$

The axial pressure drop behavior, at any value for y, takes a parabolic profile.

5. Adomian method solution

In this section, we use the Adomian method to solve nonlinear ordinary differential equation (35) with the boundary condition (36). The Adomian Decomposition Method has much attention in recent years in applied mechanics in general, and in particular the area of series. The method proved to be powerful, effective, and can easily handle a wide class of linear and nonlinear, ordinary and partial differential equations, and linear or nonlinear integral equations. The Adomian Decomposition Method was developed by George Adomian in and is well addressed in the literature [34,35].

For solving Eq. (35) we write it in operator form:

$$\begin{aligned}G&=L^{-1}(\gamma^2G^{(4)}-\gamma^2M^2G''+\alpha\,\gamma^2(yG^{(3)}+2G''))\\&\quad+R_e\gamma^2L^{-1}(GG^{(3)}-G'G'').\end{aligned} \tag{46}$$

Since $\quad L^{-1}(*)=\underbrace{\int_0^y(*)dy}_{6-times}.$

then the solution can be written as:

$$G=L^{-1}(R(G))+L^{-1}(N(G)). \tag{47}$$

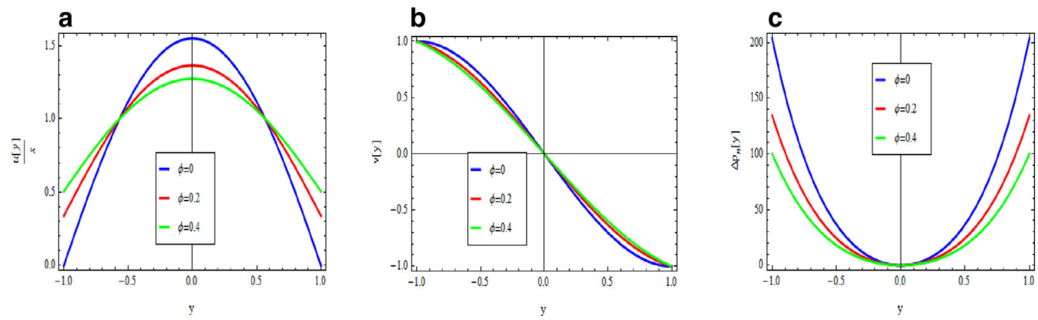

Fig. 2 Shows variation of velocity components and the normal pressure for different values of ϕ at fixed ($\gamma = 0.3,\ M = 10,\ \alpha = 0.5,\ R_e = 0.2$).

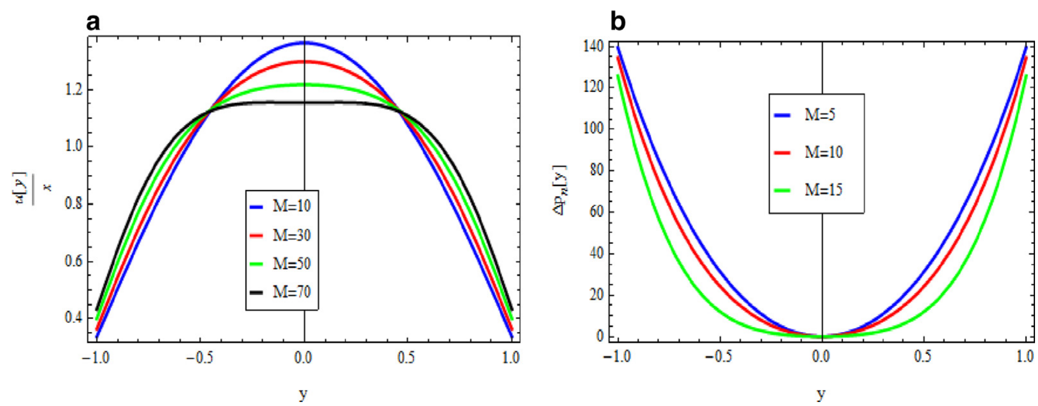

Fig. 3 Shows variation of the axial velocity and the normal pressure for different values of M at fixed ($\gamma = 0.3,\ \phi = 0.2,\ \alpha = 0.5,\ R_e = 0.2$).

Where $R(G)$ is the linear term and $N(G)$ is the nonlinear term and we get the nonlinear term from the following expression:

$$N(u) = \sum_{n=0}^{\infty} A_n(G_0, G_1, G_2, \ldots, G_n), \tag{48}$$

since

$$A_n = \frac{1}{n!}\frac{d^n}{d\zeta^n}(N(\sum_{i=0}^{n}\zeta^i G_i))|_{\zeta=0}, \quad n \geq 0. \tag{49}$$

Then the solution take the form:

$$G = \sum_{n=0}^{\infty} G_n = G_0 + L^{-1}(R(\sum_{n=0}^{\infty} G_n)) + L^{-1}(\sum_{n=0}^{\infty} A_n)), \tag{50}$$

then we get the following recursive relation:

$$\begin{aligned} &G_0 = \textstyle\sum_{j=0}^{5} m_j y^j, \\ &G_{n+1} = L^{-1}(R(G_n)) + L^{-1}(A_n), \quad n \geq 0. \end{aligned} \tag{51}$$

where m_j is integral constants for the equation $G^{(6)} = 0$ and we use the boundary condition (36) to calculate our constants. Then the solution of our problem can be written as:

$$G = \sum_{n=0}^{\infty} G_n = G_0 + G_1 + G_2 + \cdots \tag{52}$$

our solution has a big form for this we cannot write the expression of our solution.

6. Results and discussion

In this section we interpret the effect of our different physical parameters on the velocity components $\frac{u}{x}$, v and the normal pressure Δp_n.

Fig. 2 shows that effects of slip coefficient ϕ, we note that the slip coefficient has obvious influence on the axial velocity and the normal pressure. From Fig. 2a we observe that the axial velocity is decreasing as ϕ increasing at the center, which it increasing function of ϕ near to the wall, this is the same effect for [23,24] and others. Fig. 2b shows that the radial velocity is a decreasing function of ϕ. From Fig. 2c we observe that the slip coefficient has obvious influence on Δp_n near to the wall, also the normal pressure is decreasing as ϕ increasing.

When a uniform steady magnetic field acts normal to the channel walls, the structure of the flow changes drastically, as shown in Fig. 3a, also, we show that the effects of the magnetic field become more pronounced as the field increases. Even at the moderate Hartman numbers used in this project, the velocity profile is nearly straight. Hartman numbers for many industrial and laboratory applications can be large ($M = 10 - 10000$). The axial velocity is a decreasing function of M, this results agree with the physical situation such that by increasing Hartman number the Lorentz force increases which opposes the fluid motion, this result is consistent with previous results as [4].

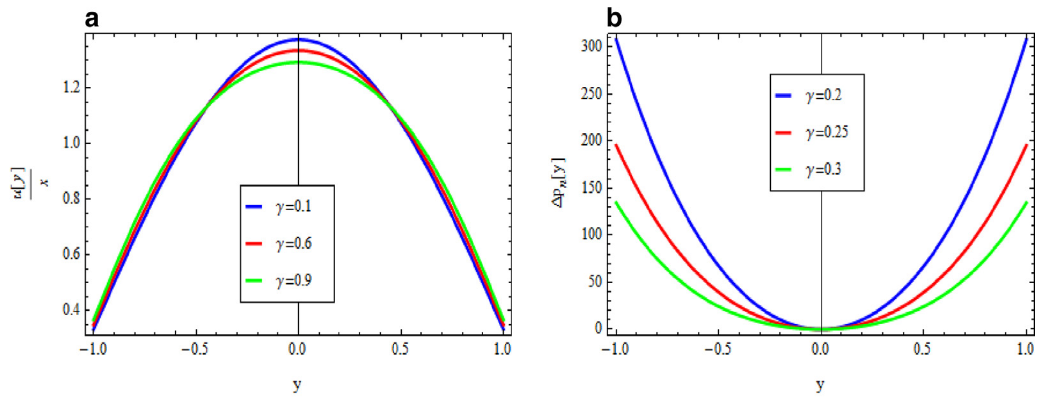

Fig. 4 Shows variation of the axial velocity and the normal pressure for different values of γ at fixed ($M = 10,\ \phi = 0.2,\ \alpha = 0.5,\ R_e = 0.2$).

Table 2 Table shows the variation of the axial velocity for different values of α at fixed ($M = 10,\ \phi = 0.2,\ \gamma = 0.3,\ R_e = 0.5, -0.5$).

y	$\alpha = -0.5$, $R_e = 0.5$	$\alpha = 0$, $R_e = 0.5$	$\alpha = 0.5$, $R_e = 0.5$	$\alpha = -0.5$, $R_e = -0.5$	$\alpha = 0$, $R_e = -0.5$	$\alpha = 0.5$, $R_e = -0.5$
−1	0.338435	0.338379	0.338322	0.336771	0.336714	0.336658
−0.8	0.668876	0.668781	0.668687	0.666133	0.666038	0.665943
−0.6	0.957788	0.957723	0.957658	0.956015	0.95595	0.955885
−0.4	1.17855	1.17857	1.17859	1.17919	1.1792	1.17922
−0.2	1.31601	1.31611	1.31621	1.31894	1.31904	1.31915
0	1.36258	1.36272	1.36286	1.36644	1.36657	1.36671
0.2	1.31601	1.31611	1.31621	1.31894	1.31904	1.31915
0.4	1.17855	1.17857	1.17859	1.17919	1.1792	1.17922
0.6	0.957788	0.957723	0.957658	0.956015	0.95595	0.955885
0.8	0.668876	0.668781	0.668687	0.666133	0.666038	0.665943
1	0.338435	0.338379	0.338322	0.336771	0.336714	0.336658

Table 3 Table shows the axial velocity for analytic and Adomian methods for different values of α and R_e at fixed ($M = 10,\ \phi = 0.2,\ \gamma = 0.3$).

y	$\alpha = 0.1, R_e = 0.2$ analytic	$\alpha = 0.1, R_e = 0.2$ adomian	$\alpha = 0.6, R_e = 0.8$ analytic	$\alpha = 0.6, R_e = 0.8$ adomian
−1	0.337867	0.337531	0.338809	0.337476
−0.8	0.667938	0.667384	0.669489	0.667292
−0.6	0.957177	0.956819	0.958176	0.956755
−0.4	1.17876	1.17889	1.1784	1.17891
−0.2	1.31701	1.3176	1.31535	1.3177
0	1.3639	1.36468	1.36173	1.36482
0.2	1.31701	1.3176	1.31535	1.3177
0.4	1.17876	1.17889	1.1784	1.17891
0.6	0.957177	0.956819	0.958176	0.956755
0.8	0.667938	0.667384	0.669489	0.667292
1	0.337867	0.337531	0.338809	0.337476

Fig. 3b clear that Hartman number has obvious effect on the normal pressure and Δp_n decreases as M increases.

The effect of the dimensionless couple stress parameter γ on axial velocity has been presented in Fig. 4a. It can be observed that the axial velocity decreases near to the central plane as the value of γ increases. However, this trend is reversed near walls. We also note that the effect of couple stresses is obvious on Δp_n and it decreases the normal pressure, as shown in Fig. 4b. Table 2 illustrates the behavior of the axial velocity for permeation Reynolds number $R_e = 0.5$, over a range of dimensionless wall dilation rate α. Table 2 describes the case of contracting and expanding wall ($-1 < \alpha < 1$) together with injection ($R_e = 0.5$). In case of expanding wall ($\alpha > 0$), the greater a, that is, the expansion ratio of the wall is, the higher shall be the axial velocity near the center, and the lower near the wall. That is because the flow toward the center become greater to make up for the space caused by the expansion of the wall and as a result the axial velocity also become greater near the center. In case of contracting wall ($\alpha < 0$), increasing contraction ratio leads to lower axial velocity near to the center, and the higher near to the wall because the flow toward the wall become greater and as a result the axial velocity near to the wall become greater. The same discussion for the suction case $R_e = -0.5$.

Finally Table 3 shows that the difference between adomian and analytical methods for solving this problem, from this table we note that the error is order of 10^{-4} for first two columns ($\alpha = 0.1,\ R_e = 0.2$) and order of 10^{-3} for others columns ($\alpha = 0.6,\ R_e = 0.8$).

7. Conclusion

A MHD for a couple stress fluid in a porous channel with expanding or contracting walls and slip boundary condition are studied in this work. The solutions for the limiting case as a $\gamma \longrightarrow \infty$, $M \longrightarrow$ and $\phi \longrightarrow 0$ (as couple stresses, magnetic field and slip coefficient approaches to zero) are obtained by Boutros et al. [28]. It is interesting to note that these limiting solutions are well in agreement with the solutions of respective problems of Newtonian uid. The most important results obtained as the following:

- For no-slip case $\phi = 0$ the fluid adheres to the walls and axial velocity is maximum at the center of the channel. By increasing the slip parameter the velocity at the channel walls increases. However, it decreases at center of the channel by increasing slip parameter.
- The axial velocity is a decreasing function of Hartman number M, these results clearly establish the fact that the fluid motion is retarded due to imposition of the transverse magnetic field.
- We also note that the effect of couple stresses is obvious for small values of γ and become a constant as γ increases (i.e. we move from a couple stress fluid to Newtonian fluid).
- In case of expanding wall ($\alpha > 0$), the axial velocity be maximum near the center. That is because the flow toward the center become greater to make up for the space caused by the expansion of the wall and as a result the axial velocity also become greater near the center.
- In case of contracting wall ($\alpha < 0$), increasing contraction ratio leads to lower axial velocity near to the center, and the higher near to the wall because the flow toward the wall become greater and as a result the axial velocity near to the wall become greater.

Acknowledgments

The author wishes to thank reviewers for their useful comments that enhance my manuscript.

Appendix A

$$s = \sqrt{\frac{\gamma^2 - \sqrt{-4M^2\gamma^2 + \gamma^4}}{2}}, \quad r = \sqrt{\frac{\gamma^2 + \sqrt{-4M^2\gamma^2 + \gamma^4}}{2}},$$

$$a_1 = \frac{s^3 \cosh[s]}{s^3 \cosh[s] f_1 - r^3 \cosh[r] f_2},$$

$$a_2 = -\frac{r^3 \cosh[r]}{s^3 \cosh[s] f_1 - r^3 \cosh[r] f_2},$$

$$a_3 = 1 - \frac{s^3 \cosh[s] \sinh[r]}{s^3 \cosh[s] f_1 - r^3 \cosh[r] f_2} + \frac{r^3 \cosh[r] \sinh[s]}{s^3 \cosh[s] f_1 - r^3 \cosh[r] f_2}$$

$$b_1 = \frac{s^3 \cosh[s] f_3 + f_4 f_2}{s^3 \cosh[s] f_1 - r^3 \cosh[r] f_2},$$

$$b_2 = -\frac{r^3 \cosh[r] f_3 + f_4 f_1}{s^3 \cosh[s] f_1 - r^3 \cosh[r] f_2},$$

$$b_3 = -\frac{(s^3 \cosh[s] f_3 + f_4 f_2) \sinh[r]}{s^3 \cosh[s] f_1 - r^3 \cosh[r] f_2} + \frac{(r^3 \cosh[r] f_3 + f_4 f_1) \sinh[s]}{s^3 \cosh[s] f_1 - r^3 \cosh[r] f_2} - f_5,$$

$$f_1 = (1 - r^2\phi) \sinh[r] - r \cosh[r], \quad f_2 = (1 - s^2\phi) \sinh[s] - s \cosh[s],$$

$$f_3 = \frac{\gamma^2 a_1}{4(2r^2 - \gamma^2)}\Big((1 + (2 + r^2)\phi) \sinh[r] + r(1 + 4\phi) \cosh[r] - \frac{(6r^2 - \gamma^2)}{r(2r^2 - \gamma^2)}(r(1 + 2\phi) \sinh[r] + r^2\phi \cosh[r])\Big) + \frac{\gamma^2 a_2}{4(2s^2 - \gamma^2)}\Big((1 + (2 + s^2)\phi) \sinh[s] + s(1 + 4\phi) \cosh[s] - \frac{(6s^2 - \gamma^2)}{s(2s^2 - \gamma^2)}(s(1 + 2\phi) \sinh[s] + s^2\phi \cosh[s])\Big),$$

$$f_4 = \frac{\gamma^2 a_1}{4(2r^2 - \gamma^2)}\Big(r(6 + r^2) \cosh[r] + 6r^2 \sinh[r] - \frac{(6r^2 - \gamma^2)}{r(2r^2 - \gamma^2)}(r^3 \sinh[r] + 3r^2 \cosh[r])\Big) + \frac{\gamma^2 a_2}{4(2s^2 - \gamma^2)}\Big(s(6 + s^2) \cosh[s] + 6s^2 \sinh[s] - \frac{(6s^2 - \gamma^2)}{s(2s^2 - \gamma^2)}(s^3 \sinh[s] + 3s^2 \cosh[s])\Big),$$

$$f_5 = \frac{\gamma^2 a_1}{4(2r^2 - \gamma^2)}\Big(\sinh[r] - \frac{(6r^2 - \gamma^2)}{r(2r^2 - \gamma^2)} \cosh[r]\Big) + \frac{\gamma^2 a_2}{4(2s^2 - \gamma^2)}\Big(\sinh[s] - \frac{(6s^2 - \gamma^2)}{s(2s^2 - \gamma^2)} \cosh[s]\Big)$$

where the other constants is very large, so we cannot write it here.

References

[1] V.K. Stokes, Couple stress in fluid, Phys. Fluids 9 (1966) 1709–1715.
[2] N. Ali, T. Hayat, M. Sajid, Peristaltic flow of a couple stress fluid in an asymmetric channel, Biorheology 44 (2007) 125–138.
[3] Kh. S. Mekheimer, Peristaltic transport of a couple-stress fluid in a uniform and non-uniform channels, Biorheology 39 (2002) 755–765.
[4] Kh. S. Mekheimer, Peristaltic flow of blood under effect of a magnetic field in a non-uniform channels, Appl. Math. Comput. 153 (2004) 763–777.
[5] E.F.E. Shehawy, Kh. S. Mekheimer, Couple-stresses in peristaltic transport of fluids, J. Phys. D. Appl. Phys. 27 (1994) 1163–1170.

[6] Kh. S. Mekheimer, Effect of the induced magnetic field on peristaltic flow of a couple stress fluid, Phys. Lett. A 372 (2008) 4271–4278.
[7] O.A. Samuel, O.K. Semiu, A.F. John, A.A. Samson, Entropy generation analysis for a reactive couple stress fluid flow through a channel saturated with porous material, Energy 93 (2015) 1239–1245.
[8] M. Turkyilmazoglu, Exact solutions for two-dimensional laminar flow over a continuously stretching or shrinking sheet in an electrically conducting quiescent couple stress fluid, Int. J. Heat Mass Transf. 72 (2014) 1–8.
[9] R. Ellahi, E. Shivanian, S. Abbasbandy, T. Hayat, Analysis of some magnetohydrodynamic flows of third order fluid saturating porous space, J. Porous Media 18 (2015) 89–98.
[10] R. Ellahi, S. Aziz, A. Zeeshan, Non Newtonian nanofluids flow through a porous medium between two coaxial cylinders with heat transfer and variable viscosity, J. Porous Media 16 (2013) 205–216.
[11] A. Zeeshan, R. Ellahi, M. Hassan, Magnetohydrodynamic flow of water/ethylene glycol based nanofluids with natural convection through porous medium, Eur. Phys. J. Plus 129 (261) (2014) 1–10.
[12] S. Uchida, H. Aoki, Unsteady flows in a semi-infinite contracting or expanding pipe, J. Fluid Mech. 82 (1977) 371–387.
[13] M. Ohki, Unsteady flows in a porous, elastic, circular tube: Part 1, the wall contracting or expanding in an axial direction, Bull. JSME 23 (1980) 679–686.
[14] N.M. Bujurke, N.P. Pai, G. Jayaraman, Computer extended series solution for unsteady flow in a contracting or expanding pipe, IMA J. Appl. Math. 60 (1998) 151–165.
[15] J. Majdalani, C. Zhou, Moderate-to-large injection and suction driven channel flows with expanding or contracting walls, Z. Ang. Math. Mech. 83 (2003) 181–196.
[16] S. Dinarvand, Viscous flow through slowly expanding or contracting porous walls with low seepage Reynolds number: A model for transport of biological fluids through vessels, Comput. Meth. Biomech. Biomed. Eng. 14 (2011) 853–862.
[17] G.S. Beavers, D.D. Joseph, Boundary conditions at a naturally permeable wall, J. Fluid Mech. 30 (1967) 197–207.
[18] V. Vand, Viscosity of solutions and suspensions, J. Phys. Colloid Chem. 52 (1948) 277–299.
[19] P.G. Saffman, On the boundary condition at the surface of a porous medium, Stud. Appl. Math. 50 (1971) 93–101.
[20] I. Isenberg, A note on the flow of blood in capillary tubes, Bull. Math. Biol. 15 (1953) 149–152.
[21] T.T. Zhang, L. Jia, Z.C. Wang, X. Li, The application of homotopy analysis method for 2-dimensional steady slip flow in microchannels, Phys. Lett. A 372 (2008) 3223–3227.
[22] J.I. Ramos, Asymptotic analysis of channel flows with slip lengths that depend on the pressure, Appl. Math. Comput. 188 (2007) 1310–1318.
[23] A. Riaz, S. Nadeem, R. Ellahi, A. Zeeshan, Exact solution for peristaltic flow of Jeffrey fluid model in a three dimensional rectangular duct having slip at the walls, Appl. Bionics Biomech. 11 (2014) 81–90.
[24] A.A. Khan, R. Ellahi, M. Usman, The effects of variable viscosity on the flow of non-Newtonian fluid through a porous medium in an inclined channel with slip conditions, J. Porous Media 16 (2013) 59–67.
[25] A. Zeeshan, R. Ellahi, Series solutions of nonlinear partial differential equations with slip boundary conditions for non-Newtonian MHD fluid in porous space, Appl. Math. Inf. Sci. 7 (2013) 257–265.
[26] H. Stephani, M. MacCallum, Differential Equations: Their Solutions using Symmetries, Cambridge University Press, Englewood Cliffs, Cambridge, 1989.
[27] L.V. Ovsianniko, Group Analysis of Differential Equations, Cambridge Academic Press, New York, 1982.
[28] Y.Z. Boutros, M.B. Abd-el Malek, N. Badran, H.S. Hassan, Lie–group method solution for two-dimensional viscous flow between slowly expanding or contracting walls with weak permeability, Appl. Math. Model. 31 (2007) 1092–1108.
[29] Kh. S. Mekheimer, S.Z.A. Husseny, A.T. Ali, R.E. Abo-Elkhair, Lie group analysis and similarity solutions for a couple stress fluid with heat transfer, J. Adv. R. Appl. Math. 2 (2010) 1–17.
[30] Kh. S. Mekheimer, S.Z.A. Husseny, A.T. Ali, R.E. Abo-Elkhair, Lie point symmetries and similarity solutions for an electrically conducting Jeffrey fluid, Phys. Scr. 83 (2011) 015017.
[31] Kh. S. Mekheimer, S.Z.A. Husseny, A.T. Ali, R.E. Abo-Elkhair, Similarity solution for flow of a micro-polar fluid through a porous medium, Appl. Appl. Math. 6 (2011) 2082–2093.
[32] Kh. S. Mekheimer, M.F. El-Sabbagh, R.E. Abo-Elkhair, Lie group analysis and similarity solutions for hydro-magnetic maxwell fluid through a porous medium, Bound. Value Probl. 2012 (2012) 1–18.
[33] F. Shahzad, M. Sajid, T. Hayat, M. Ayub, Analytic solution for flow of a micropolar fluid, Acta Mech. 188 (2007) 93–102.
[34] G. Adomian, Solving Froniter Problems of Physics: The Decomposition Method, Kluwer Academic Publishers, Boston, 1994.
[35] G. Adomian, A review of the decomposition method in applied mathematics, J. Math. Anal. Appl. 135 (1988) 501–544.